STUDY ON CONCEPTS FOR RADAR INTERFEROMETRY FROM SATELLITES FOR OCEAN (AND LAND) APPLICATIONS

Studie zu Konzepten für Radar-Interferometrie über Ozeanen (und Land) im Rahmen zukünftiger Satellitenmissionen

(KoRIOLiS)

SECTION 3: CURRENT MEASUREMENTS

Roland Romeiser and Donald R. Thompson

Direct surface current measurements are a particularly appealing oceanic application of (along-track) InSAR, since they cannot be obtained from any other type of spaceborne instrument. In this section we discuss potential applications and the advantages of InSAR compared to other instruments, we describe imaging mechanisms and techniques for the retrieval of currents from InSAR data, and we analyze the dependence of the results on radar parameters and environmental parameters, as well as accuracies and spatial resolutions that can be achieved.

3.1. MOTIVATION

Information on oceanic currents is very valuable for a number of applications, as documented, for example, in the EuroGOOS Data Requirements Survey report [*Fischer & Flemming*, 1999]. EuroGOOS is an association of European national agencies for developing operational oceanographic systems and services in European seas, and for promoting European participation in the Global Ocean Observing System (GOOS). It was founded in 1994. Within the framework of EuroGOOS, a comprehensive data requirements survey was carried out to get an overview of operational marine data requirements of 155 organizations in six European countries.

From a list of 136 oceanic variables such as current velocity, deep ocean salinity, heat flux, etc., the surface current velocity and direction were the two most requested ones: 60% of the respondents are interested in information about these parameters. Furthermore, 39% are interested in coastal bathymetry (which can, to some extent, be determined from measured current fields), 23% in geostrophic currents (which could be determined from ATI or XTI data), 19% in eddies, jets, and fronts, and 10% in sea ice motions (which can be determined from InSAR phase, intensity, and coherence images in various ways).

Regarding the resolution in space and time, most of the respondents of the EuroGOOS questionaire who are interested in open ocean currents request a spatial resolution on the order of 1 km and a temporal resolution of hours to days, depending on the application. For monitoring coastal bathymetry, the spatial resolution should be better than 1 km, and the requested temporal resolution ranges from hours to more than one year.

3.1.1. Promising Applications

Interferometric current measurements from satellites could satisfy a considerable portion of the EuroGOOS user requirements. Unique properties of a spaceborne InSAR would be its capability to provide repeated quasisynoptic current measurements over thousands of square kilometers with a spatial resolution on the order of 100 m, as well as its global coverage (within a few days). The latter could be useful for validating or updating circulation models, but the high resolution of SAR would not be required for this application. Furthermore, conventional along-track interferometry (ATI) would provide only one component of the surface current, while circulation models deal with three-dimensional current vectors for the whole water column, which can vary in complex ways. Finally, the acquisition of large amounts of SAR data over the open ocean can be difficult due to limitations in data downlink and onboard storage capacities.

Current measurements by InSAR appear to be most promising for coastal applications: Relatively small amounts of data, which could be received through existing ground stations, would cover a major part of the coastlines and coastal waters whose observation has highest priority for practical applications such as monitoring of bathymetric changes, pollution, and river outflows, as well as ship routing and regional circulation modeling. A high spatial resolution of 50 to 100 m would be fully exploited by these applications. Moreover, vertical variations of the current field within the water column are often negligible in coastal waters, and measurements of only one component of the current field can be sufficient for applications such as bathymetry retrieval.

3.1.2. Alternatives to InSAR

For a complete understanding of the advantages and disadvantages of current measurements by InSAR, one should be aware of potential alternatives:

- Acoustic Doppler current profilers (ADCPs) are the most common in-situ sensors for oceanic currents. They provide measurements of three-dimensional current vectors for the whole water column, and they can reside on the bottom for many days and thus provide long time series of data. Main shortcomings of ADCPs are that they are not well suited for surface current measurements (wave motions etc. at the water / air interface cause large errors) or for synoptic measurements over large areas (arrays of many instruments would be required). Furthermore, instrument deployment and retrieval can be difficult and time consuming, and the data from bottom-mounted devices are not immediately accessible for near-real-time analysis.

- Conventional synthetic aperture radar (SAR) systems have been in space for many years and have proven to be quite useful for a variety of oceanic applications. Current features such as fronts, jets, eddies, and internal waves, as well as the spatially varying tidal currents over underwater bathymetry can become visible in SAR intensity images via hydrodynamic modulation of the surface roughness (see, for example, the paper by *Alpers* [1995]). This imaging mechanism is quite well understood, and sophisticated theoretical models and model inversion schemes have been developed. However, nonlinearities and complex feedback schemes in the SAR imaging mechanism, as well as a strong dependence of the SAR signatures on parameters which are not very well known, such as the wind speed and direction, can make the quantitative interpretation of SAR signatures of current features very difficult and ambiguous [*Romeiser et al.*, 2001]. ATI would be much better suited for this purpose, since it provides actual current measurements, and the imaging mechanism is much more direct than the SAR intensity imaging mechanism of current features.
- Another well-proven instrument for oceanography from space is the radar altimeter, which provides information on geostrophic currents via measurements of the sea surface topography over scales of tens to thousands of kilometers (see, for example, the paper by *Wunsch & Stammer* [1998]). However, the data processing is quite complicated, and the measuring principle as well as the coarse resolution of several kilometers make the technique unsuitable for coastal applications. Radar altimetry and (along-track) SAR interferometry complement each other rather than competing.
- Coastal HF radar is a remote sensing instrument for coastal current and wave measurements which is usually operated from the shore (see, for example, the paper by *Essen et al.* [2000]). State-of-the-art HF radar systems have a maximum range on the order of 60 km and a spatial resolution of about 300 m or worse. HF radar permits synoptic two-dimensional current measurements with a high temporal resolution of about 10 minutes and over long periods. Main disadvantages compared to ATI are the relatively coarse resolution and limited spatial coverage. HF radar may be better suited for applications such as a continuous monitoring of current and wave fields in river estuaries and areas of high ship traffic, while InSAR has clear advantages for monitoring bathymetric changes and pollution and for other applications that require current measurements with high spatial resolution and wide coverage.
- Also nautical radars can, to some extent, be used for current measurements. This technique is based on the distortion of the dispersion shells of frequency-wavenumber spectra of long ocean waves in the presence of mean currents, which can be detemined from time series of radar images [*Senet et al.*, 2001]. However, the two-dimensional current vectors obtained this way are averaged over large areas or long times, and the spatial resolution and coverage are very limited.

We conclude that the main advantages of spaceborne InSAR for oceanic applications, compared to other sensors, would be its capability to provide synoptic current measurements over large areas with high spatial resolution and its wide coverage.

3.2. CURRENT MEASUREMENTS BY ATI

Pure along-track interferometry (ATI) is the classical concept for current measurements by synthetic aperture radar, which was originally proposed by *Goldstein & Zebker* [1987]. ATI exploits the fact that the phase of microwave backscatter from a moving target changes with time at a rate which is determined by the line-of-sight target velocity (this effect corresponds to the Doppler shift in frequency). Two complex SAR images of a scene which are acquired with a short time lag will exhibit a phase difference proportional to the time lag and to the rate of phase change. Accordingly, the phase difference can be converted into a target velocity. However, first surface current fields computed this way from ATI phase images from the 1989 Loch Linnhe experiment deviated significantly from in-situ data [*Thompson & Jensen*, 1993]. Improved ATI imaging models had to be developed, which account for contributions of sub-resolution-scale surface wave motions to the ATI phase signatures.

3.2.1. ATI Imaging Mechanism of Currents

A comprehensive theory of the ATI imaging of ocean current features was presented by *Thompson & Jensen* [1993]. It accounts for contributions of the phase velocities of the two Bragg wave components (short ocean waves which are in resonance with the microwave signal and which are propagating in and against the radar look direction) and of the orbital velocities of longer waves to the observed ATI phases, as well as for effects of the hydrodynamic modulation of the surface wave spectrum by spatially varying currents. Based on this approach, *Thompson & Jensen* [1993] were able to reproduce basic properties of observed ATI signatures from the 1989 Loch Linnhe experiment quite well. However, their way of converting ocean wave spectra into microwave Doppler spectra by using the model by *Thompson* [1989] was

quite time consuming, and their numerical scheme for the computation of hydrodynamically modulated ocean wave spectra was not designed for application to large two-dimensional current arrays.

Romeiser & Thompson [2000] presented a simplified model for the simulation of Doppler spectra, which does not require time-dependent calculations and is thus faster than the model by *Thompson* [1989] by an order of magnitude or even more. A comparison showed that, despite totally different approaches, the two models produce very similar results. Due to better numerical efficiency, the simulations discussed in the following have been carried out with the SAR / InSAR imaging model of the University of Hamburg, also known as the M4S model, whose along-track InSAR module is based on the theory by *Romeiser & Thompson* [2000].

3.2.1.1. Model Description

The M4S model consists of a wave-current-wind interaction module, which computes the modulation of the ocean wave spectrum by given current and / or wind fields, and a radar module for the conversion of the spatially varying wave spectra into normalized radar backscattering cross sections (NRCS), Doppler spectra, SAR intensity images, InSAR phase and coherence images, etc. Both modules have been highly optimized for computational efficiency and user friendlyness, so that they can be applied to a variety of scenarios without dedicated adaptation and produce simulated SAR or InSAR images within reasonable computation times.

The wave-current interaction module is basically described in the paper by *Romeiser & Alpers* [1997]. It computes the modulation of the complete two-dimensional ocean wave spectrum by a spatially varying current field on the basis of weak hydrodynamic interaction theory in a relaxation time approach. Later additions include the capability to deal also with spatially varying wind fields [*Ufermann & Romeiser*, 1999a,b] and to account for higher-order modulation effects such as a surface roughness - wind stress feedback mechanism [*Romeiser et al.*, 1999] or wave breaking.

The radar module of the M4S model is described in detail in the papers by *Romeiser et al.* [1997] and by *Romeiser & Thompson* [2000]. It is a composite surface model based on Bragg scattering theory [*Valenzuela*, 1978], which accounts for the effect of longer waves by means of a Taylor expansion of the NRCS and of other quantities up to second order in the surface slopes parallel and normal to the radar look direction. Second-order terms of the NRCS are obtained, which are proportional to the mean square surface slopes. Corresponding expressions are also obtained for the mean Doppler offset and for the Doppler bandwidth. Furthermore, the azimuthal displacement of signatures of moving targets in SAR images is taken into account, and InSAR phases and coherences can be computed as well as realizations of single-look or multi-look intensity and phase images with correct statistical properties.

Altogether, the following phenomena are taken into account in ATI simulations with the M4S model:

- the contribution to the phase difference image which corresponds to the actual surface current field to be measured;
- the effect of the phase velocity of the two Bragg wave components propagating towards and away from the radar and the asymmetric weighting of their contributions to the Doppler spectrum due to differences in wave intensity;
- contributions of longer waves, which result from correlated variations of the local NRCS and the line-of-sight component of the orbital velocity;
- spatial variations of the contributions of Bragg waves and longer waves, which result from the hydrodynamic modulation of the wave spectrum by spatially varying currents and, if applicable, variations in the wave spectrum with the local wind; and
- artifacts of the SAR imaging mechanism, such as an azimuthal displacement of targets which have a velocity component in the line-of-sight direction, velocity bunching, etc.

3.2.1.2. Model Validation

The feasibility of explaining differences between uncorrected "interferometric velocities" and actual surface currents by contributions of wave motions and their spatial variations was demonstrated quite successfully by *Thompson & Jensen* [1993]. Another test case was a comparison between corrected ATI-derived currents and HF radar data by *Graber et al.* [1996]. Again, good agreement was found. *Romeiser & Thompson* [2000] demonstrated that Doppler spectra obtained from the M4S model are consistent with those from the more fundamental model by *Thompson* [1989], which had been validated against L and K_u data from experiments. Furthermore, the wave-current interaction module of the M4S model produces similar results as the one used by *Thompson & Jensen* [1993] and by *Graber et al.* [1996] (the models are

based on the same fundamental equations), and it has been applied successfully to a number of test cases [e.g. *Romeiser et al.*, 1997; *Ufermann & Romeiser*, 1999a,b; *Romeiser et al.*, 1999]. It thus appears to be justified to use the M4S model also for theoretical sensitivity analyses of the ATI imaging mechanism of current fields [see also *Romeiser & Thompson*, 2000] and for simulations of data products of future InSAR systems.

Figure 3-1 shows the location of three bottom-mounted ADCPs and the flight pattern of an airborne X-band ATI system during the first EURoPAK experiment, which took place in the German Bight in April 1999. Altogether, four flights were performed in the morning and in the afternoon of April 27 and 28, 1999. The ATI data were converted into currents by using M4S model results (see also 3.2.2.). Figure 3-2 shows a comparison of the ATI results, ADCP data, and predictions of a numerical circulation model, which exhibit good overall agreement.

Figure 3-1: Test site of the first EURoPAK experiment in the German Bight of the North Sea, north of the island Heligoland (April 1999). Red dots indicate locations of three bottom-mounted ADCPs deployed by the German Federal Maritime and Hydrographic Agency, and green lines indicate flight tracks and directions of the airborne X-band ATI system of Aero-Sensing GmbH.

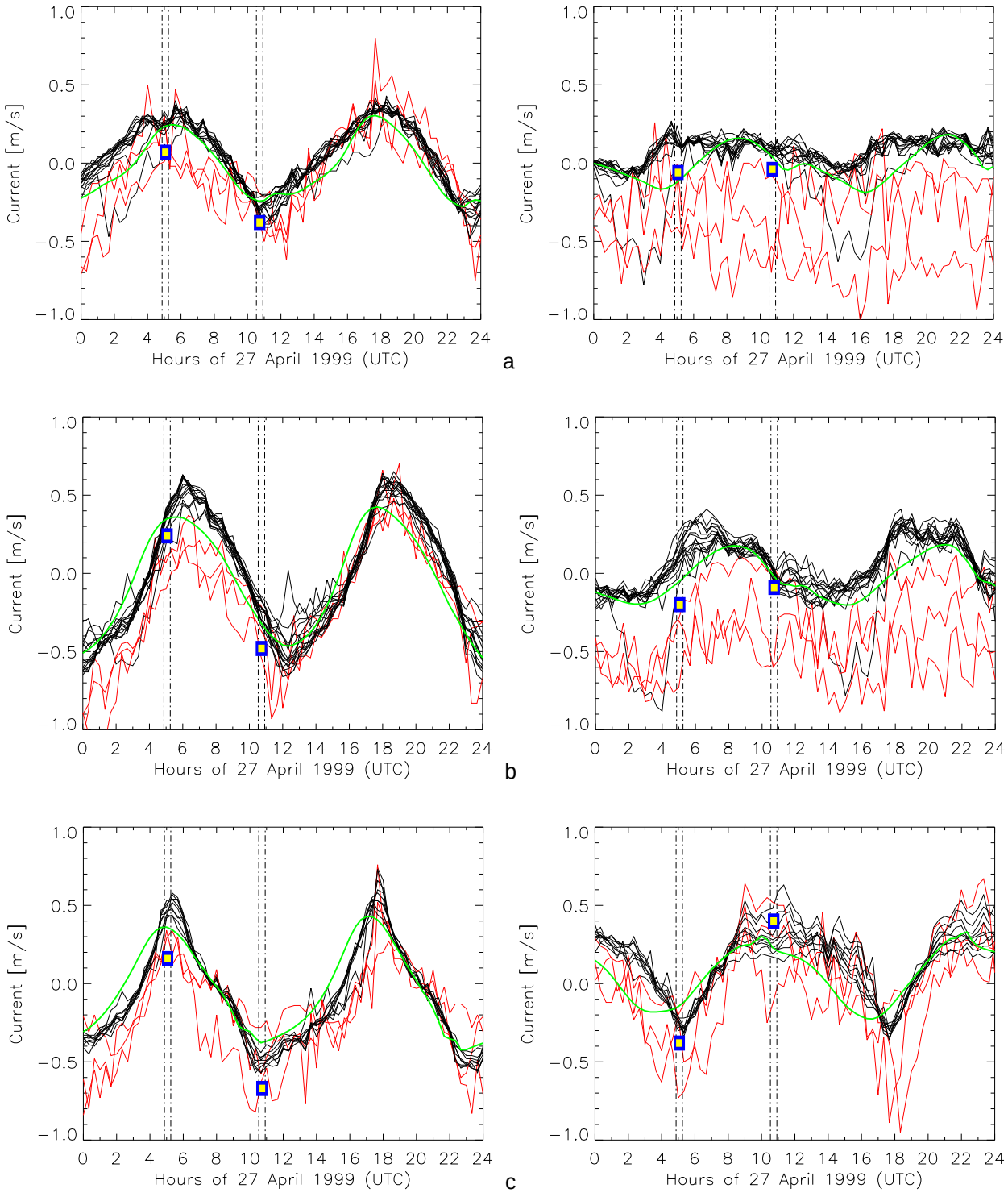

Figure 3-2: Comparison of currents measured by ADCPs (red curves: upper three depth bins; black curves: lower bins), computed by a circulation model of the German Federal Waterways Engineering and Research Institute (green lines), and obtained from airborne ATI data with corrections according to the M4S model (yellow-blue squares); the three rows (a), (b), (c) correspond to the three ADCP locations; left and right columns correspond to x and y components of the current.

3.2.2. Current Retrieval Technique

Due to the required corrections for wave motion effects, the conversion of ATI phase images into current fields is less straightforward than originally expected. However, the relation between an ATI phase image and the corresponding array of line-of-sight velocity components is much more linear than the relation between any other data product from spaceborne sensors and ocean currents. We show in the following two subsections what inversion scheme should be used to retrieve current fields from ATI phase images and how the results can be further refined by including additional SAR and ATI data products in the data processing algorithm.

3.2.2.1. Conversion of ATI Phase Images into Current Fields

Before discussing the proposed algorithm for the conversion of ATI phase images into measured surface current fields and its advantages, we would like to revisit the corresponding algorithm for current retrieval from SAR intensity images and the difficulties associated with it (see *Romeiser et al.* [2001] for a detailed discussion on this topic). Figure 3-3 shows a schematic overview.

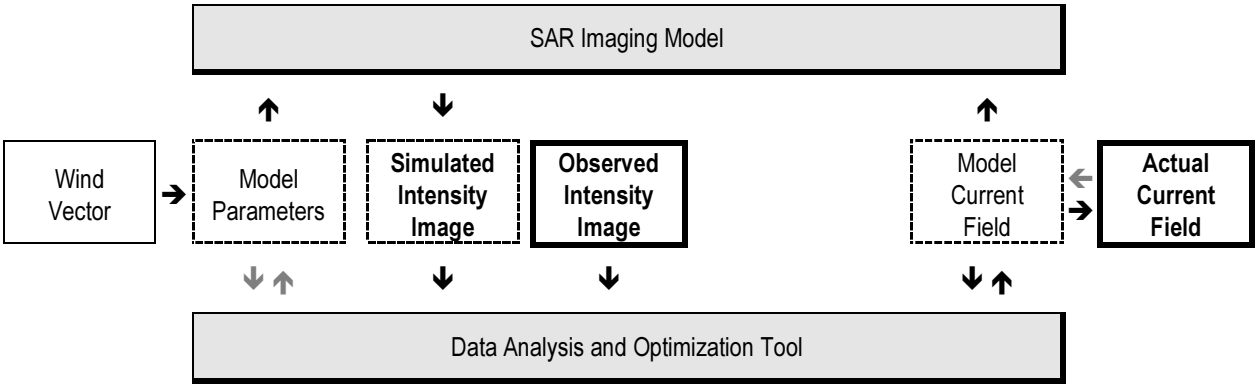

Figure 3-3: Scheme of a typical algorithm for the retrieval of surface currents from SAR intensity images [after Romeiser et al., 2001].

The main problem with SAR intensity signatures in this context is that not the currents themselves, but current gradients are imaged via hydrodynamic modulation of the surface roughness (wave-current interaction). Furthermore, the imaging mechanism includes a number of nonlinearities and can depend strongly on environmental parameters such as the wind vector. Thus direct inversion is impossible. In the general case, not even a first-guess current field can be obtained from a SAR intensity image alone. Additional information from external sources, such as tide tables, analytical or numerical models of the phenomenon, or in-situ measurements, must be used. This way, some assumptions on the current field to be retrieved from the SAR data enter into the algorithm from the beginning, and the final result is not independent of this a-priori information. This is symbolized by the gray arrow on the right of the diagram of Figure 3-3, which makes the "actual current field" not only an output quantity, but also – to some extent – an input quantity.

Once a first-guess current field is obtained, a corresponding SAR image can be computed by a numerical SAR imaging model and compared with the observed SAR image. The latter is done by a data analysis and optimization algorithm, which modifies the model current field in such a way that better agreement between the simulated and the observed SAR image can be expected after another model run. After a number of iteration cycles, a model current field is obtained which leads to the best possible agreement, and this current field is the best estimate of the actual current field and thus the output of the algorithm.

Since SAR intensity signatures depend not only on the input current field but also on the wind vector and the ambient ocean wave spectrum, which are usually not known with high accuracy, differences between simulated and observed SAR images do not necessarily result from shortcomings of the model current field. In fact, even a correct current field and correct environmental parameters will not necessarily result in a perfect reproduction of the observed SAR image by a model, since also the available models have certain shortcomings and are not suited for operational application to any kind of scenario. One must conclude from these problems and the problems to obtain a first-guess current field that the retrieval of current fields from SAR intensity images is difficult and that the accuracy and spatial resolution which can be achieved are quite limited.

In contrast to this, the ATI imaging mechanism is much less sensitive to environmental parameters, and it is much more linear. In principle, an ATI phase image can be converted into a first-guess model current field by simple multiplication with a proportionality factor and correction for the mean contribution of wave motions, which can be computed easily. Corrections for the effect of spatially varying wave intensities (as a result of wave-current interaction) are much smaller than in the case of SAR intensity images and can be made within a few iteration cycles. Also corrections for SAR / ATI mapping artifacts (azimuthal shift, velocity bunching) can be applied during this procedure. A schematic overview of the current retrieval algorithm for ATI phase images is shown in Figure 3-4. Even if wind vectors are not very well known and the ATI imaging model is not perfect, the ATI phase image inversion is much more robust and accurate than the inversion of a SAR intensity image under ideal conditions.

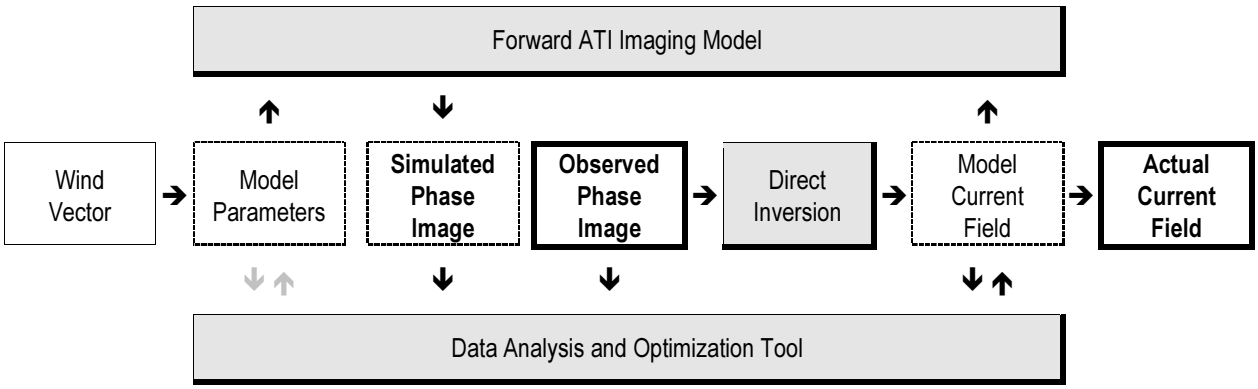

Figure 3-4: Scheme of the proposed algorithm for the retrieval of surface currents from ATI phase images.

The differences between SAR intensity signatures and ATI phase signatures of spatially varying currents are nicely illustrated by plots in the paper by *Romeiser & Thompson* [1999], which are reproduced in Figure 3-5. The plots show simulated P-band (0.45 GHz) SAR intensity (NRCS) signatures and X-band (10 GHz) ATI phase signatures (converted into "ATI currents" without any correction) of a typical current field over underwater sandwaves near the Dutch coast for two different wind directions. The two frequency bands were selected such that the SAR intensity and the ATI phase are as linear as possible in the surface current gradient and in the current itself, respectively. However, the simulated P-band SAR intensity signatures are still related to the current in a complicated, nonlinear way and change drastically with the wind direction. In contrast, the shape of the ATI phase signatures resembles the shape of the current variations closely in both cases. The main difference between actual currents and ATI currents is a constant offset, which results from contributions of wave motions to the phase signatures and which varies with the wind direction. If the wind speed vector is known, the data can be corrected for this offset easily.

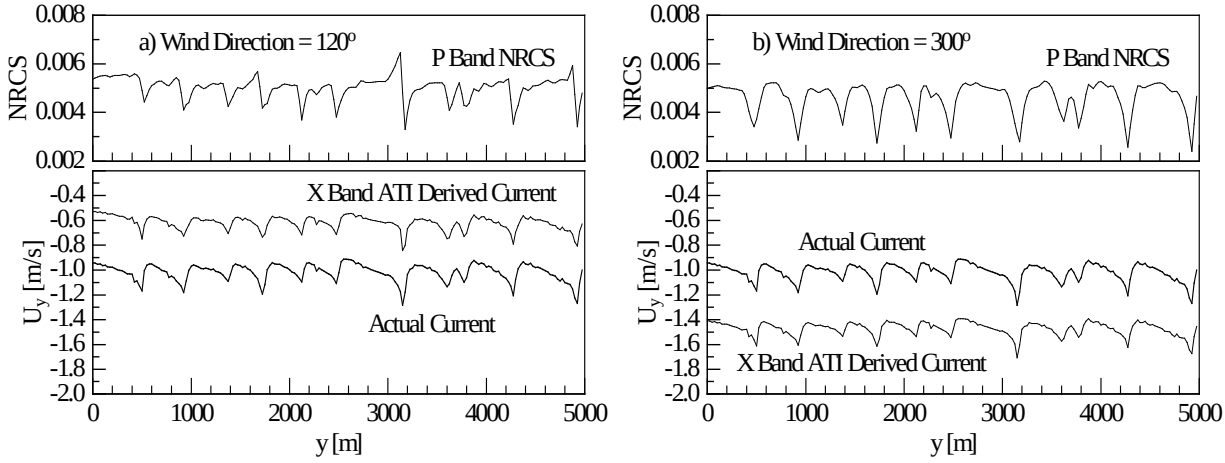

Figure 3-5: Typical surface current over underwater sandwaves near the Dutch coast (bold line) and simulated P-band SAR intensity signature (upper plot) and X-band ATI phase signatures (converted into "ATI currents" without corrections; narrow line in lower plot); wind speed is 7 m/s; wind direction is 120° (a) and 300° (b) with respect to the x axis [from Romeiser & Thompson, 1999].

3.2.2.2. Use of Additional Data Products

Together with the phase image, which is the main data product for current measurements, ATI provides conventional SAR intensity images and (with additional processing) coherence images, which can be exploited to obtain additional information and to refine the results of the imaging model inversion. Ideally, not only the observed phase signatures, but also SAR intensity and coherence signatures should be reproduced by the ATI imaging model when the final solution for the current field is obtained. Discrepancies between data and model results may indicate a problem such as, for example, incorrect assumptions on the wind field or the ambient ocean wave spectrum. A correction can result in considerable improvement of the current field retrieval. SAR intensity and coherence can also help to obtain information on the current component perpendicular to the line of sight, since they are more sensitive to variations in this component than the ATI phase (see also 3.2.6). Figure 3-6 shows an example of a current field and simulated ATI phase, SAR intensity, and coherence signatures. The different characteristics of the signatures are clearly visible. For comparison, all quantities (except the input current field) are shown in grayscales.

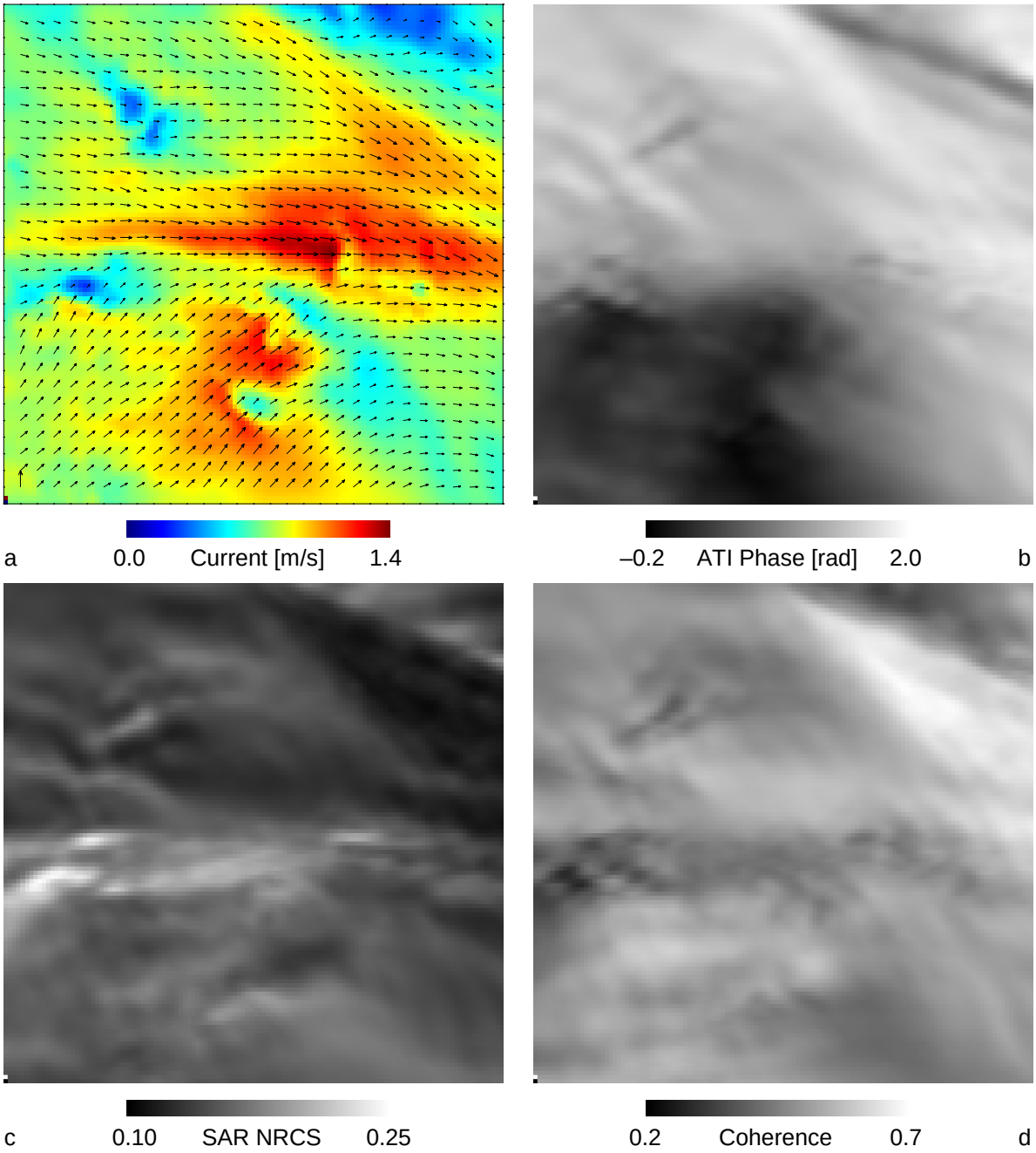

Figure 3-6: Input current field (a) and simulated (expectation value) ATI phase image (b), SAR intensity (NRCS) image (c), and coherence image (d); radar frequency = 5.3 GHz, polarization = VV, incidence angle = 30°, look direction = from bottom to top of the figures; wind = 6 m/s from top left to bottom right; test area size = 3000 m × 3000 m.

If the measured SAR image intensities are calibrated (which can be assumed for a spaceborne SAR), they can be used to determine the wind vector, which is an important parameter for the current retrieval, from the ATI dataset itself. Procedures for wind retrieval from SAR images are described, for example, in the papers by *Horstmann et al.* [2000, 2001]. On images which include land (sandbanks, beaches), the coherence can be used as a sensitive parameter for the classification of land and water, i.e. coastline detection, since it is much smaller for water than for hard targets (see section 2.1).

3.2.2.3. Experimental Results

An inversion scheme for ATI data according to Figure 3-4 has been implemented at the University of Hamburg within the framework of the research project EURoPAK. The test site and the flight pattern of the first EURoPAK experiment at the island Heligoland were already shown in Figure 3-1, and a comparison of the ATI-derived current vectors with ADCP data from three locations was shown in Figure 3-2. We will now illustrate the data processing in more detail by showing some intermediate-level products.

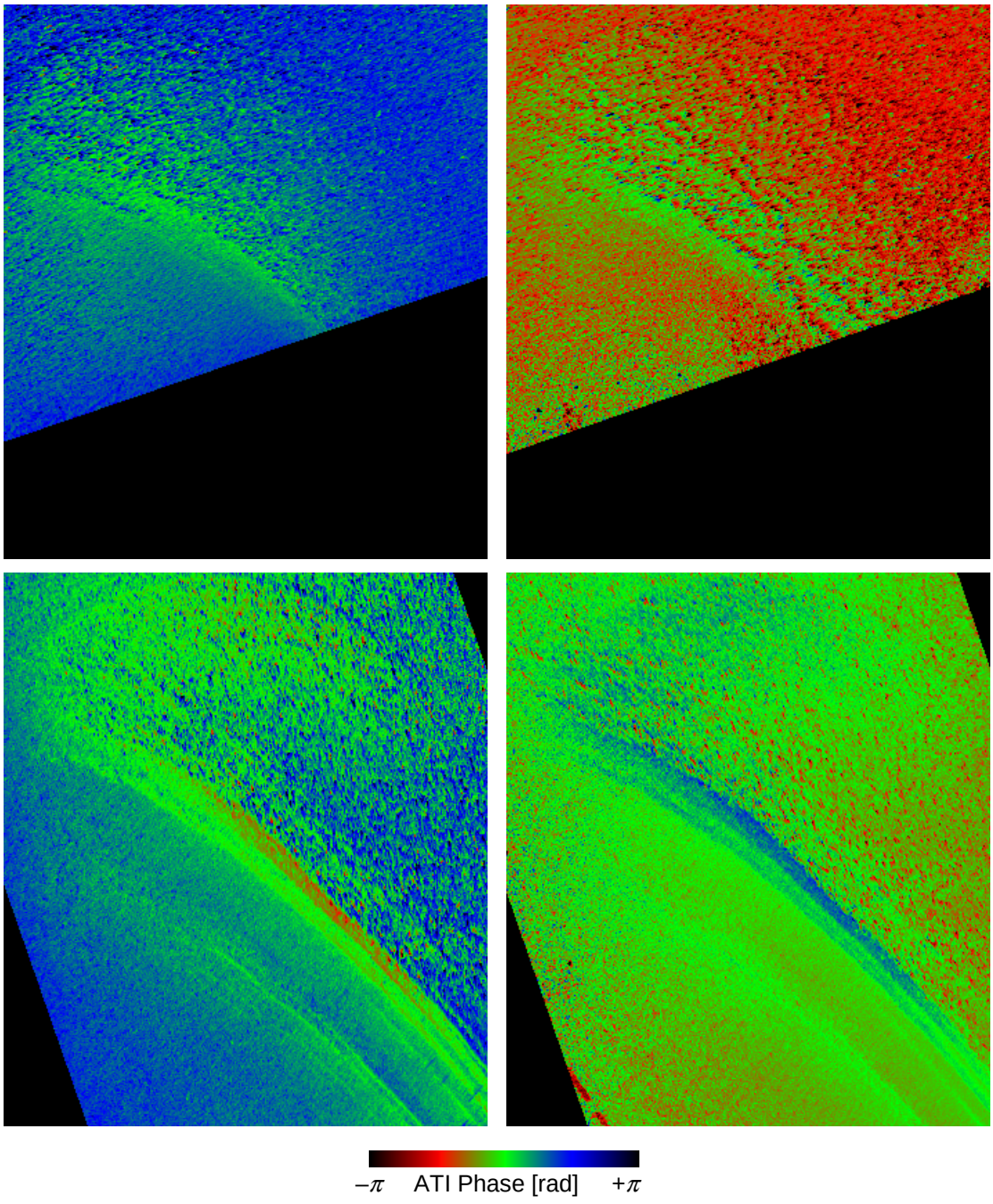

Figure 3-7: ATI phase images from the four legs of the EURoPAK flight pattern at Heligoland shown in Figure 3-1; first flight on April 27, 1999, 5:00 UTC; area size: 3500 m $\times$ 4000 m.

Figure 3-7 shows ATI phases obtained from the four legs of the flight pattern shown in Figure 3-1, as obtained during the first flight on April 27, 1999, 5:00 UTC. One can clearly see the modulation of the surface velocity pattern by the underwater reef. The phase signatures from opposite look directions appear reversed and at the same locations, which is an expected result, offering a good opportunity for a first quality and consistency check. In general it is not necessary to acquire pairs of ATI images from opposite look directions. Only two perpendicular look directions are always desirable to obtain a full two-dimensional measurement (see also 3.2.6). However, an advantage of multiple measurements of the same velocity component is the fact that stationary contributions (on time scales of at least several minutes) can be distinguished from the instationary ones resulting from long surface waves which are resolved by the radar. The images of Figure 3-7 exhibit clear signatures of such waves. A correlation filter was developed, which separates correlated and uncorrelated variations in a pair of phase images. Only the correlated contributions enter into the ATI current field.

Before applying the correlation filter, the phase images are corrected for SAR imaging artifacts (the azimuthal displacement of targets in the ATI image can be determined from the phase) and averaged over 20 m $\times$ 20 m (approx. 100 looks). After applying the correlation filter, phases are corrected for mean contributions of wave motions as obtained from the M4S model and converted into the first solution for the surface current. This current field, together with the final solution, which was obtained after several iteration cycles of the optimization scheme of Figure 3-4, is shown in Figure 3-8.

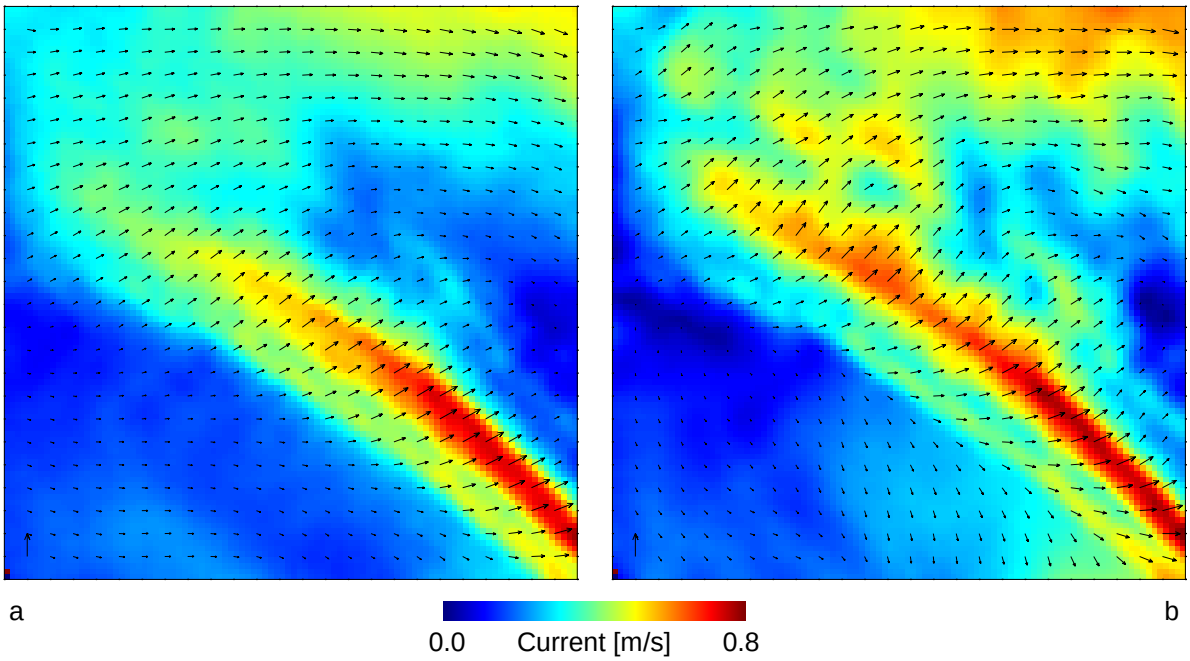

Figure 3-8: Surface current field derived from the data of the first EURoPAK flight (Figure 3-7), before (a) and after (b) applying corrections for spatially varying wave contributions; area size: 2000 m $\times$ 2000 m.

The main goal of the project EURoPAK has been the development of a remote sensing technique for underwater bathymetry on the basis of ATI and SAR images. Figure 3-9 shows an example result for the Heligoland test site. A full depth map with the grid spacing of the ATI-derived current field (20 m $\times$ 20 m) was obtained by correlating 218 known depths from echosoundings (line spacing = 400 m) with the corresponding measured current vectors and deriving a regression line between currents and depths, which was then used to determine depths at all grid points from the measured currents. Tests with various subsets of the full echosounder dataset of 1018 data points (100 m line spacing) indicated that the depth retrieval algorithm is quite robust and works even if the available depth data cover only a small sub-interval of the total range of depths in the test area, and that the results are realistic and reliable.

3.2.3. Effect of Radar Parameters

A comprehensive study on the dependence of ATI signatures of current fields on a variety of radar parameters and environmental parameters (based on model simulations) was presented by *Romeiser & Thompson* [2000]. In the following, we summarize the most important findings from their paper and other publications and show some examples of model results.

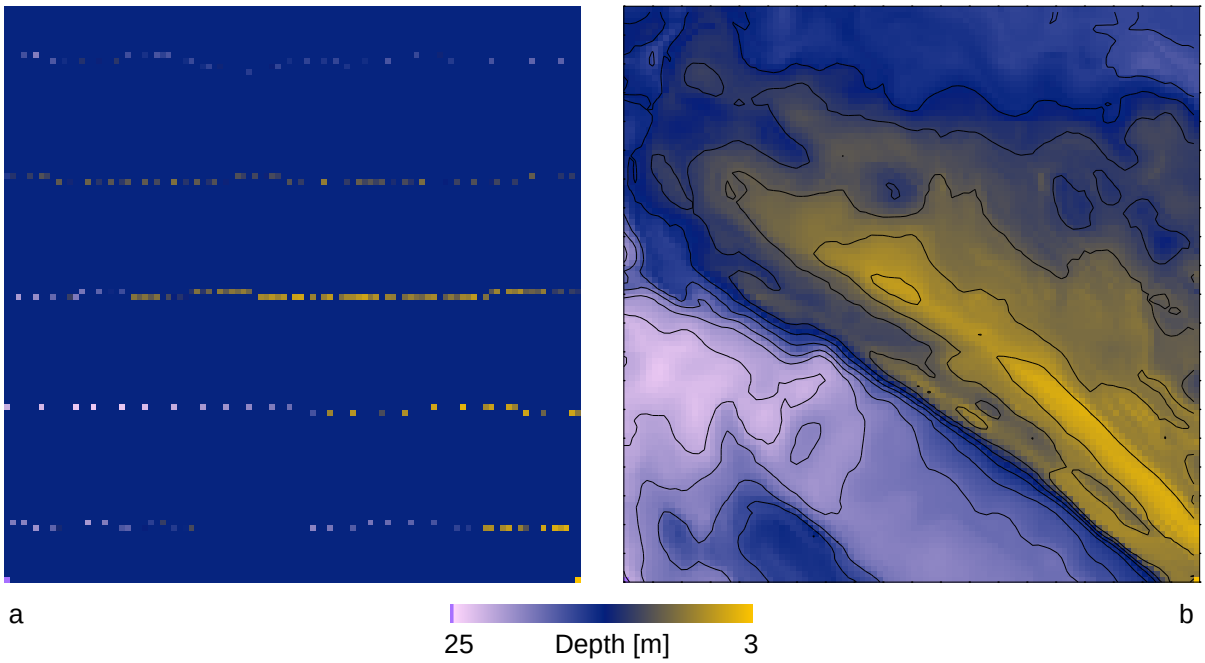

Figure 3-9: 218 data points from echosoundings (a; line spacing = 400 m) and bathymetric map (b) obtained by correlating the ATI-derived current field of Figure 3-8b with these data.

3.2.3.1. Radar Frequency

According to *Thompson & Jensen* [1993], high microwave frequencies are preferable for current measurements by ATI, since the hydrodynamic modulation of the two Bragg wave components is less pronounced and less asymmetric at short wavelengths than at longer wavelengths, which should lead to a more linear imaging of spatially varying currents. Although this is correct, the simulated ATI signatures at L- and X-band by *Romeiser & Thompson* [2000] do not indicate the expected clear advantage of higher frequencies. The strong hydrodynamic modulation of the decimeter waves which act as Bragg waves at L-band enters also into the simulated ATI signatures at X-band via higher-order effects. Some advantage of X-band with respect to L-band may result from the fact that the dependence of the mean ATI phase and, thus, the wind-induced mean offset of the ATI-derived current on the wind direction is less pronounced. However, if reasonable wind data are available and a state-of-the-art radar imaging model is used, the radar frequency does not appear to be a critical parameter for successful current measurements by ATI. More important in this context are the dependence of the useful range of ATI time lags on the radar frequency (see section 2) and other technical constraints which are discussed in section 5. For example, the choice of the radar frequency may determine the need for a single-platform or a multi-platform design.

3.2.3.2. Polarization

Also the polarization of the ATI system is not a critical parameter from a model inversion point of view – simulated ATI signatures of current gradients are found to be very similar at vertical (VV) and horizontal (HH) polarization. However, the NRCS of the ocean is higher at VV than at HH by a few dB, which results in a better signal-to-noise ratio (SNR) at VV. This can be important at low wind speeds, where the NRCS of the ocean may be close to the noise equivalent NRCS of the radar. Accordingly, the preferred polarization for radar interferometry over the ocean is VV. The least favorable choice is cross polarization (HV or VH), where the NRCS would be even lower than at HH by several dB. Multi-polarization capabilities can be useful for the interpretation of SAR intensity signatures, because differences between intensity signatures at different polarizations can be exploited for the classification of current-induced and wind-induced NRCS variations and thus for the determination of the wind field from the data. Fully polarimetric capabilities are not particularly useful for oceanic applications.

3.2.3.3. Incidence Angle

In order to obtain clear signatures of surface current variations, the incidence angle of an ATI system should be as high as possible: At steep incidence angles, the relative contribution of vertical components of orbital wave motions to the ATI signatures is large, and the variation of this contribution with the hydrodynamic modulation of the waves leads to strong nonlinearities in the imaging mechanism. An example of simulated X-band ATI signatures of a model current field at incidence angles of 30° and 60° from nadir [from *Romeiser & Thompson*, 2000] is shown in Figure 3-10.

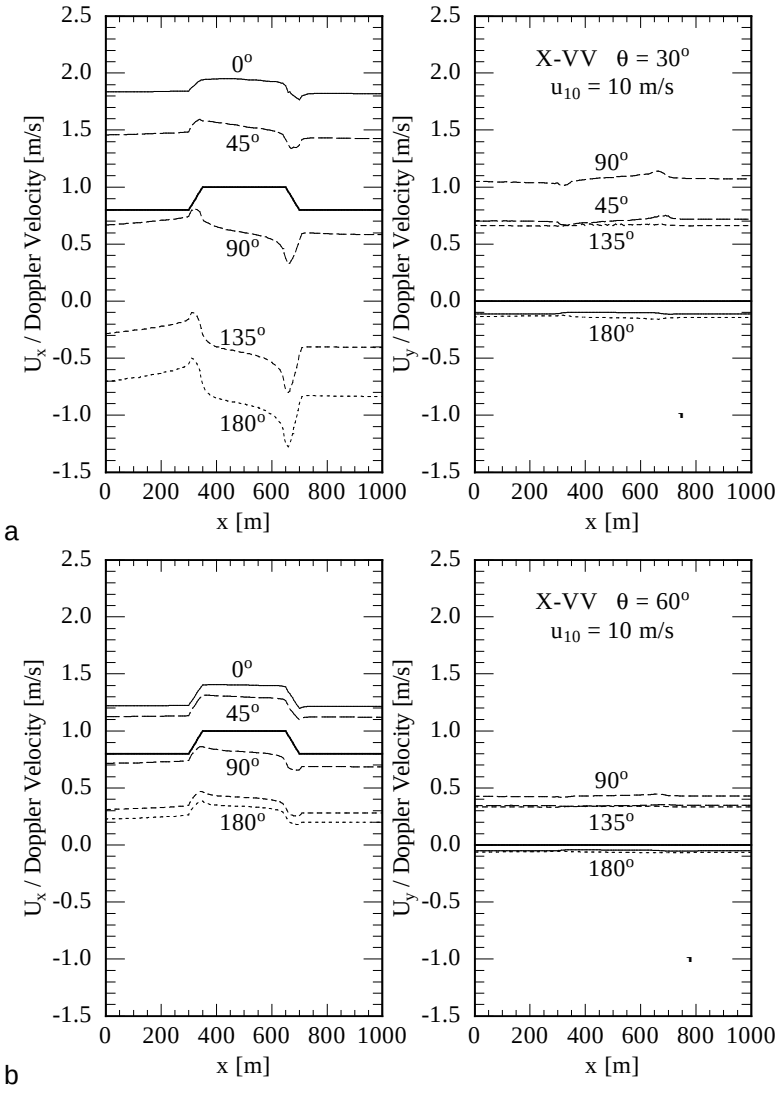

Figure 3-10: x and y components (left and right plot) of a model current field (bold lines) and of corresponding simulated "Doppler velocities" (velocities equivalent to the Doppler shift of the radar signal, thin lines) for different wind directions; X-band (10 GHz), wind speed = 10 m/s; incidence angle = 30° (a) and 60° (b) [from Romeiser & Thompson, 2000].

However, the NRCS of the ocean decreases strongly with increasing incidence angle, which leads to a decreasing SNR and decreasing coherence. Ideal incidence angles for current measurements by ATI with reasonable nonlinearities and reasonable coherence should be between about 35° and 45°.

3.2.3.4. Antenna Separation / Baselines

For a discussion on the dependence of the coherence and the sensitivity of an ATI system for current measurements on the ATI and XTI baselines, see section 2.

3.2.3.5. R/V Ratio

The ratio of the distance between radar antenna and target (R) and the platform velocity (V) determines the nonlinearity of the SAR imaging mechanism, i.e. the magnitude of the azimuthal displacement of targets with a line-of-sight velocity component in SAR and ATI intensity and phase images. For a spaceborne SAR, the velocity is determined by the orbit altitude and cannot be selected independently. At the typical altitude of 800 km and the corresponding velocity of 7000 m/s and for an incidence angle of 45°, the R/V ratio is on the order of 160 s. Figure 3-11, which has also been adopted from the paper by *Romeiser & Thompson* [2000], depicts the effect of the SAR imaging artifacts for a spaceborne ATI (i.e., R/V = 160 s) and, for comparison, for an airborne ATI with an R/V ratio of 60 s (altitude = 3000 m, velocity = 100 m/s, incidence angle = 60°) on the phase signatures of a simple model current feature. For R/V = 160 s, the nonlinearities are quite pronounced. This must be taken into account when converting phase images into current fields, but the effect is well understood and can be reproduced by numerical SAR and ATI imaging models in the ATI current algorithm.

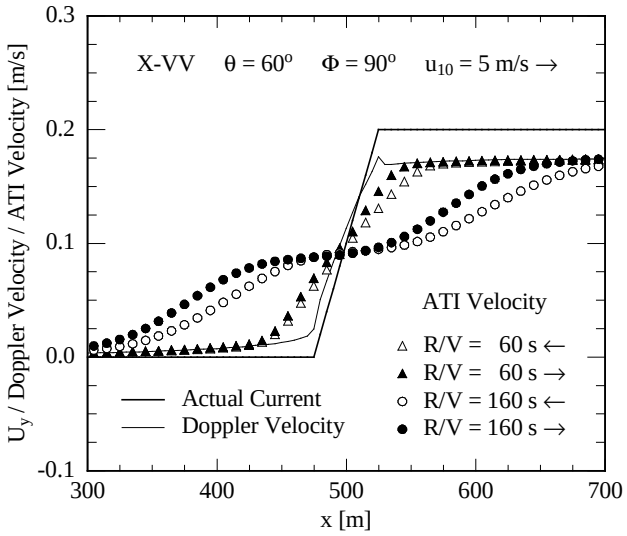

Figure 3-11: Model shear current ("oceanic front") in range direction and simulated Doppler velocity signatures (without SAR imaging artifacts) and ATI velocity signatures (with SAR imaging artifacts) for different values of R/V and for flight directions to the left and to the right; radar frequency = 10 GHz, incidence angle = 60°, wind speed = 5 m/s [from Romeiser & Thompson, 2000].

3.2.4. Effect of Environmental Parameters

The wind and wave conditions at oceanic test sites cannot be optimized for ATI measurements, but the sensitivity of different ATI configurations to wind and wave conditions may be different, and one can discuss the effect of this sensitivity on the capabilities and limitations to measure currents.

3.2.4.1. Wind Speed

A high wind speed leads to a large NRCS and reduced hydrodynamic modulation of the Bragg waves, which is desirable for clear ATI signatures, but it can also increase the intensity ratio of the two Bragg wave components – thus the wave-induced mean offset of the ATI signatures – and the intensities of longer waves – thus the higher-order contributions to ATI phase images and the corresponding nonlinearities in the imaging mechanism. According to the model results by *Romeiser & Thompson* [2000], the dependence of ATI signatures on the wind speed is not very pronounced, and a clear advantage of low or high wind speeds is not found. Examples are shown in Figure 3-12. However, the simulations by *Romeiser & Thompson* [2000] produce "expectation value" results, which correspond to ensemble averages over many realizations. An ATI phase image from an actual experiment will exhibit signatures of the nonstationary orbital motion patterns of long ocean waves which are resolved by the radar (see section 4). Filtering techniques need to be applied to extract the current field from such data (see 3.2.2.3). Accordingly, the presence of long ocean waves of large amplitude can lead to a decrease of the achievable spatial resolution of the current field retrieval. As a rule of thumb, the peak wavelength of the ocean wave spectrum (in meters) is on the order of the wind speed (in m/s) squared. That is, the peak wavelength for a wind of 10 m/s is on the order of 100 m, and it will be difficult to determine current variations with a spatial resolution better than the peak wavelength from a single ATI image. The lowest useful wind speed for current measurements by ATI is determined by the condition that the NRCS of the ocean needs to be significantly larger than the noise equivalent NRCS of the radar system.

3.2.4.2. Wind Direction

The wind direction with respect to the radar look direction affects the intensity ratio of the two Bragg wave components propagating towards and away from the radar and thus the mean offset of the ATI currents with respect to the true currents. Furthermore, the wind direction has an effect on longer waves and their hydrodynamic modulation and thus on the corresponding nonlinearities of the imaging mechanism. This effect, as well as the dependence of the ATI signatures on the magnitude of the wind speed, is depicted by the plots of Figure 3-12. Note the strong variation of the shape of the ATI signatures with the wind direction (which would be less pronounced at higher incidence angles). In order to correct the data for these nonlinearities, exact knowledge of the wind vector is essential. The most linear imaging of currents by ATI is usually obtained for a wind direction parallel to the current, which minimizes the wave-current interaction times and thus the hydrodynamic modulation of the dominant wave components.

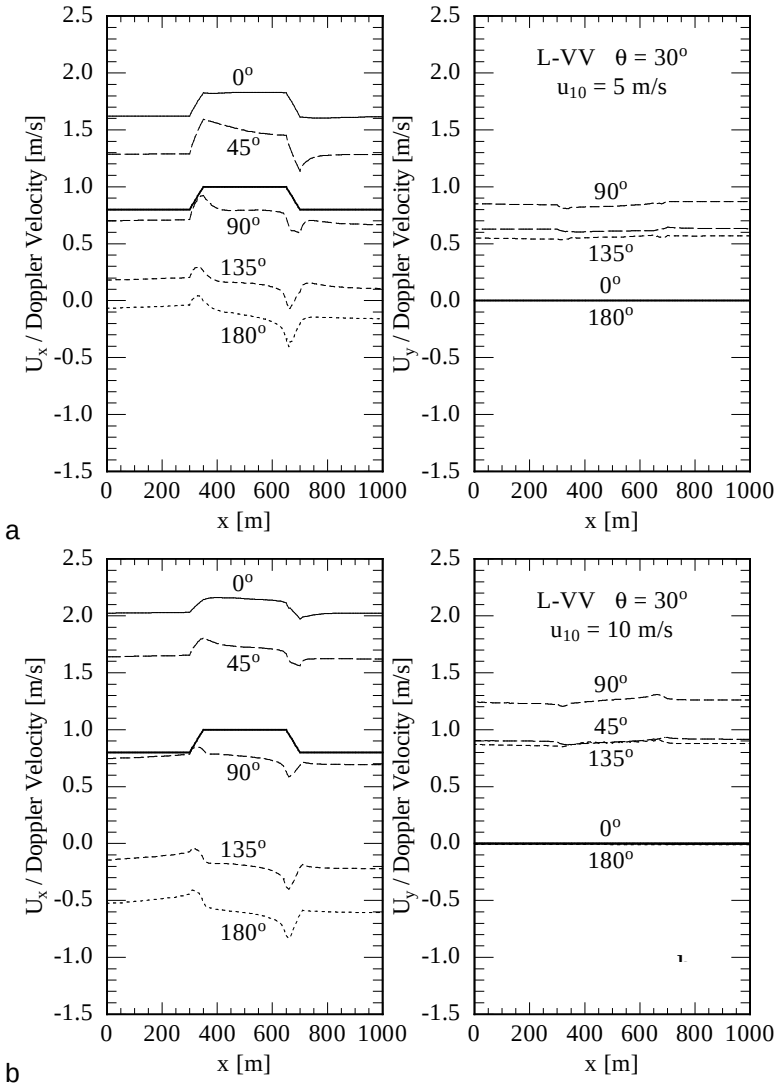

Figure 3-12: Same as Figure 3-10, but for L-band (1 GHz), an incidence angle of 30°, and wind speeds of 5 m/s (a) and 10 m/s (b) [from Romeiser & Thompson, 2000].

3.2.4.3. Wave Spectrum

In the model simulations within the current retrieval scheme (see 3.2.2), one will usually assume that the equilibrium ocean wave spectrum is determined by the wind vector, according to a standard parameterization. This assumption may be not justified under certain conditions such as, for example, when the wind has changed significantly just before an ATI image was taken, when swell waves in the test area originate from a source outside the test area, in the presence of turbulence in the atmosphere or the water, or in coastal areas with special wind / wave conditions. Unrealistic assumptions on the equilibrium wave spectrum can result in significant errors in the ATI-derived current fields. One should be aware of this problem and try to obtain as much information on local wave (and wind) conditions as possible. To some extent, the wave spectrum can be determined from the ATI data themselves – see section 4.

3.2.5. Accuracy and Spatial Resolution

Assuming that the wind vector is known and that reasonable ATI system parameters and data processing techniques are used, the conversion of ATI data into measured current fields should work very well and with small remaining uncertainties. A look at the plots of Figures 3-10 and 3-12 and experience from experiments (see, for example, Figure 3-2) indicates that it should usually be possible to obtain a bias (difference between mean ATI-derived current and mean actual current) on the order of 0.1 m/s or better and an even better accuracy of "relative" measurements, i.e. measured differences between the currents at two locations in a test area.

However, limitations of the accuracy of the current measurements and, in particular, of the spatial resolution result from the noise statistics of the data (see section 2) and from problems with non-stationary signatures such as signatures of long ocean waves (see 3.2.4.3). The confidence interval of measured

phase differences can be determined from the coherence, and it can be improved by averaging over a number of pixels. The signatures of long ocean waves must be removed by filtering, which is easier if data from multiple overflights are available. Altogether, we estimate that a spatial resolution on the order of 100 m and an RMS accuracy of measured current variations better than 0.1 m/s (in addition to a possible bias on the same order of magnitude) are realistic performance goals of spaceborne ATI systems for oceanic applications.

3.2.6. How to Measure Two-Dimensional Currents from Space

The standard configuration of an ATI system can only measure velocity components in range direction. To obtain a two-dimensional measurement of the surface current field, data from two or more overflights with different look directions can be combined (see, for example, the flight pattern of Figure 3-1), but this is practically impossible with spaceborne systems: Of course one can try to combine data from ascending and descending tracks over a test area, which have sufficiently different look directions almost everywhere. But due to a long separation in time on the order of several hours to days and the corresponding changes in the tidal phase, in wind and wave conditions, and, perhaps, in the location and strength of nonstationary phenomena such as fronts, internal waves, or eddies, one will usually not be able to measure two components of the same current field, and the combination of the data will not lead to a physically meaningful result. But there are ways of measuring two components of the surface current with one overflight, and for some applications one does not even need two-dimensional measurements. Some possible solutions to the problem are summarized in the following.

3.2.6.1. Dual-Beam ATI

The velocity component measured by an ATI system is not necessarily the component in the direction perpendicular to the flight direction, but it is the component parallel to the effective radar look direction. For example, if an airborne SAR is flown with a squint angle of 10° with respect to the nominal heading, the ATI phase is sensitive to velocities in a direction of about 80° instead of 90° from the flight direction. *Frasier & Camps* [2001] propose to exploit this effect by using two sets of InSAR antennas with beams squinted in different directions in such a way that fully two-dimensional surface current measurements can be obtained with a single overflight. According to their simulation results, the angle between the two antenna look directions may be as large as 90°. A drawback of the dual-beam design is the need for additional antennas or beam steering capabilities. A dual-beam InSAR cannot be designed as an add-on to an existing conventional, side-looking SAR system.

To some extent, one can obtain measurements in (slightly) different look directions by splitting the beam of a single-beam InSAR and processing the data from the forward and aft halves independently. However, the sensitivity of this technique to along-track velocity components is very limited – see also section 5.

3.2.6.2. "Spotlight" Mode

Another way to obtain vector current measurements would be a "spotlight" mode operation of the radar. In this case, the direction of a single beam is rotated electronically or mechanically in such a way that a target is illuminated for a longer period during the overflight from different directions. Of course, also this concept requires specially designed hardware components. Furthermore, the spatial coverage would be limited to isolated spots along the satellite track which need to be selected in advance, while a dual-beam ATI system would provide continuous coverage of large areas if necessary.

3.2.6.3. Utilization of Statistics and Hydrodynamic Models

For some applications, independent measurements of two current components at different times, which can be obtained from ascending and descending overflights, can be sufficient, since it is not necessary to obtain a snapshot of the two-dimensional current field at one instant. For example, oceanographers may want to get an idea of the long-term mean flow pattern in an area or a map of the variability of the current field within a given period. Such information can be obtained from an InSAR system with a single look direction. Under certain conditions, one can even compute the along-track component of the current field at the time of an InSAR overflight from the measured component and additional information from other sources or flow models. For example, if the bottom topography of a coastal area is known and a quasi-two-dimensional flow pattern can be assumed (i.e. the depth averaged current does not differ significantly from the surface current), one can often determine the unknown current component from the measured one by applying fundamental equations of hydrodynamics.

3.2.6.4. Use of Single-Component Current Measurements

Finally, one should be aware of the fact that there are many applications for which measurements of a single current component are sufficient. The main advantages of InSAR in this context would be its wide coverage with high spatial resolution. This applies, for example, to studies of phenomena with a quasi-one-dimensional flow pattern and a known current direction, such as rivers or oceanic internal waves, or to phenomena with a well-known symmetry, such as eddies. Also the correlation technique for bathymetric measurements with ATI (see 3.2.2.3) will, in most cases, work on the basis of a single current component.

3.3. CURRENT MEASUREMENTS BY XTI

Cross-track interferometry (XTI) uses two SAR antennas which are separated in the direction perpendicular to the flight track. In this case, phase differences depend on the topography of the illuminated area. Accordingly, XTI is mainly used for the generation of digital elevation models (DEMs) of land surfaces. There is no direct imaging of the velocity of moving targets. However, over water, an XTI system can be operated as an altimeter and measure variations in the sea level which are associated with mesoscale current phenomena.

3.3.1. XTI Imaging Mechanism of Currents

Due to the rotation of the Earth, objects which are moving along the Earth's surface experience a lateral force called Coriolis force, which is oriented "toward the right" on the northern and "toward the left" on the southern hemisphere. In strong jets in the ocean such as the Gulf Stream, the Coriolis force is balanced by the pressure differential caused by a corresponding sea level difference between both sides of the jet. This phenomenon is called geostrophy. Under geostrophic balance, the east (x) and north (y) components of the surface slope are given by

$$\frac{\partial \zeta}{\partial x} = \frac{2\Omega \sin \phi}{g} U_y \tag{3-1}$$

and

$$\frac{\partial \zeta}{\partial y} = -\frac{2\Omega \sin \phi}{g} U_x \tag{3-2}$$

where ζ is the surface elevation, Ω is the angular frequency of the Earth's rotation, ϕ is the geographical latitude, g is the gravitational acceleration, and U_x and U_y are the depth-averaged horizontal current components in x and y direction. For a current of 1 m/s at a latitude of 45°, one obtains a surface slope on the order of 10^{-5}, i.e. one centimeter per kilometer. If such surface slopes can be measured, one can calculate the corrresponding "geostrophic" currents. Also oceanic eddies and other phenomena are associated with characteristic surface slopes.

3.3.2. Current Retrieval Technique

In order to measure ocean currents with an XTI system, methods of radar altimetry must be adopted. We discuss the prospects and limitations of this approach, and we compare the capabilities of XTI and conventional radar altimetry.

3.3.2.1. XTI Altimetry

To measure sea level variations associated with current phenomena, an accuracy on the order of 1 cm is desirable. Assuming that a typical spaceborne XTI system maps an elevation range of 100 to 1000 m into a phase interval of 2π and that the accuracy of phase difference measurements is on the order of 1° (0.017 rad), the accuracy of the elevation measurement at a single pixel is not better than about 0.3 to 3 m. However, this error can be reduced by a factor $\sqrt{N}$ by averaging over N pixels. That is, one must average the measured phase differences over about 900 to 90000 pixels to arrive at the desired error level. If the spatial resolution of the SAR is 25 m, this corresponds to averaging over 750 m $\times$ 750 m to 7500 m $\times$ 7500 m. Even in the latter case, the spatial resolution of the XTI data would be comparable with the one of a conventional radar altimeter, and it would satisfy users' needs (see section 3.1).

The interpretation of the measured sea level variations in terms of currents and other phenomena must basically be done in the same way as with conventional radar altimeter data, as described, for example, in the paper by *Wunsch & Stammer* [1998].

3.3.2.2. Differences between Conventional Radar Altimetry and XTI Altimetry

Accordingly, XTI could provide at least the same accuracy and spatial resolution as a conventional radar altimeter. A unique advantage of XTI in this context would be its lateral resolution: While conventional altimeters obtain only a series of point measurements along the satellite's ground track, a SAR can have a swath width of 100 km or more. This way, an XTI system could provide a two-dimensional synoptic view of sea level anomalies within a range of about 100 km with a single overflight, while altimeter data from many ascending and descending overpasses would be required to obtain a comparable amount of information. Accordingly, the temporal resolution of the measurements could be improved enormously by using XTI. Furthermore, the data processing and interpretation would be easier. Another advantage of XTI results from its measuring principle: A conventional radar altimeter determines the sea level from the travel time of radar pulses from the antenna (whose location is well known) to the sea surface and back to the antenna. Corrections for the dependence of the speed of light on a number of atmospheric parameters are essential, some of which are on the same order of magnitude as the required accuracy of the final result. In contrast to this, XTI determines target elevations from phase differences between two signals which travel along almost the same path. Atmospheric conditions have only a small effect on this kind of measurement. A shortcoming of the XTI technique, however, is the fact that it provides only relative measurements of differences between the surface elevations at two points, but no absolute measurements. This may cause problems with measurements of sea level variations on large scales (several 100 kilometers).

3.3.3. Effect of Radar Parameters

In contrast to the ATI imaging mechanism of surface currents, the XTI imaging mechanism of surface elevations does not depend on the radar frequency or other radar parameters in complicated ways. Technically, an XTI system which works for topographic mapping over land will also be suited for oceanic measurements. The main problem in this context may be the fact that the NRCS of the ocean can be smaller than typical NRCS values of land surfaces, which may lead to SNR problems. Again, VV is the preferred polarization, because the NRCS is higher than at HH or HV / VH.

3.3.4. Effect of Environmental Parameters

The accuracy of conventional radar altimetry can suffer from effects of the so-called "sea state bias", i.e. a bias of measured sea levels in the presence of high waves, which results from the fact that the NRCS-weighted mean elevation of the backscattering facets at the crests and the troughs of long waves is not equal to their actual mean elevation. According to simulations with the M4S model, this effect should be much less pronounced for XTI measurements, where the scattering mechanism is different (Bragg scattering instead of specular reflection) and where the backscattered power is dominantly coming from facets which are tilted towards the radar and not from wave crests and troughs. Also the dependence of XTI-derived sea levels on the wind speed and direction should be practically negligible.

3.4. CURRENT MEASUREMENTS BY COMBINED ATI / XTI

Some of the concepts for spaceborne interferometric SARs which are currently being discussed, such as the "Interferometric Cartwheel" [*Massonnet*, 1999; *Massonnet et al.*, 2000; *Ramongassié et al.*, 2000] (see also section 6) are no pure along-track or cross-track InSARs but combinations of both, which usually results from technical constraints. For the generation of digital elevation models (DEMs) over land, an additional time lag between the acquisition of two XTI images does not matter, since the signal decorrelates very slowly and the targets are not moving. It is even possible to do repeat-pass interferometry with images from single-antenna SAR systems acquired with a temporal separation on time scales of years. One can argue that, in turn, a cross-track antenna separation should not affect current measurements by ATI since the ocean surface can be assumed to be flat and the XTI contribution to phase differences would just result in an additional range-dependent offset. However, the combination of along-track and cross-track baselines, which would even be time-dependent in case of the "Cartwheel", is one of the main challenges associated with spaceborne SAR interferometry from a data processing and data interpretation point of view, and a fundamental discussion of this problem has been one of the key objectives of the project KoRIOLiS.

3.4.1. Combined ATI / XTI Imaging Mechanism of Currents

As discussed in section 2, one must be aware of the problem that radar backscatter from the ocean decorrelates much faster than radar backscatter from land, thus a combined ATI / XTI system which is designed for topographic measurements over land will not necessarily work over the ocean. Also the cross-track separation of the antennas can lead to a decorrelation of the received signals; thus the coher-

ence between the signals received by two antennas of a combined ATI / XTI system can be worse than in case of a pure ATI system with the same along-track baseline if no compensation for this effect is applied in the SAR processing (see 2.1.2).

If an along-track baseline is present, one will try to measure currents by ATI rather than by XTI, since only ATI can take full advantage of the high spatial resolution of a synthetic aperture radar in this context (see sections 3.2 and 3.3). Accordingly, a combined ATI / XTI system for current measurements should be considered as ATI system with an additional cross-track antenna separation, and the main problems to be discussed are the effect of the additional cross-track baseline on the phase signatures, the magnitude of this effect, and strategies for the separation of ATI and XTI contributions.

Fortunately, the solution to these problems appears to be simple. As discussed in section 4, the elevation of ocean surface waves is imaged by XTI in a similar way as their orbital velocity is imaged by ATI. Variations of the ATI phase with the orbital velocity and variations of the XTI phase with the elevation can be related to the complex amplitude of an ocean wave by two complex phase modulation transfer functions (MTFs). For a combined ATI / XTI system, the effective total phase MTF is given by the sum of the ATI and XTI phase MTFs, which usually have different magnitudes and different phases. Accordingly, different signatures of long surface waves will be found in pure ATI, pure XTI, and combined ATI / XTI phase images of a scene. However, the mean contribution of the waves to InSAR signatures of current phenomena must be computed by weighting the phase variations with variations of the NRCS along each wave component. Since the XTI phase MTF and the MTF which describes NRCS variations are usually out of phase by an amount close to $\pi/2$, and since the XTI phase variations along a wave are, for typical ATI and XTI configurations, much smaller than the corresponding ATI phase variations, one finds that the XTI contributions of waves to mean InSAR phase signatures are smaller than their ATI contributions by some orders of magnitude and, thus, practically negligible.

3.4.2. Current Retrieval Technique

Accordingly, current fields can be retrieved from combined ATI / XTI data by the same techniques as from pure ATI data (see 3.2.2). The only particular effect which needs to be taken into account is a range-dependent additional phase offset corresponding to the XTI signature of a flat surface, which should be removed from the data before an ATI current field is derived. Also the XTI altimetry technique, as described in section 3.3, can be applied to combined ATI / XTI data. However, in this case one must take into account that the ATI baseline leads to significant mean contributions of wave motions to the InSAR phase image, which needs to be corrected for this effect.

3.5. SUMMARY

Our main findings on oceanic current measurements by spaceborne interferometric synthetic aperture radar can be summarized as follows:

- InSAR offers a unique potential to measure surface current fields from space with high spatial resolution and wide coverage. Results of user requirements surveys indicate that there is considerable demand for such data. InSAR is most promising for coastal applications, where its high resolution can be fully exploited for a variety of applications, and where its limitations to measurements of a single component of the surface current are a less critical problem than in the open ocean.
- The most promising technique for current measurements by InSAR is along-track interferometry (ATI), which permits direct measurements of line-of-sight velocities at high spatial resolution. Since the measured velocities include contributions from wave motions, corrections must be applied to determine actual surface currents from ATI data, but the ATI imaging mechanism of surface currents is well understood and much more linear than, for example, the conventional SAR intensity imaging mechanism. We propose an iterative scheme for the conversion of ATI phase images into measured current fields, which accounts for the hydrodynamic modulation of the ocean wave spectrum by surface current gradients and the corresponding spatial variations of the contributions of waves to ATI signatures, and which corrects ATI-derived current fields for this effect.
- Current measurements by ATI have been demonstrated in several experiments in Europe and the USA. The results are consistent with theoretical predictions. They have been validated against in-situ data, coastal HF radar data, and circulation model predictions. The results of these studies as well as theoretical estimates indicate that an accuracy on the order of 0.1 m/s for the mean current in range direction and better than this for relative variations is a realistic performance goal for spaceborne ATI, as well as a spatial resolution on the order of 100 m.

- Theoretical sensitivity analyses indicate that the choice of the radar frequency band does not have a strong impact on the linearity of the ATI imaging mechanism of surface currents and thus on the measuring accuracy. Also the polarization of the radar is not a critical parameter with respect to the data interpretation, but VV should be chosen in order to get the highest possible backscattered power. The incidence angle should be between about 35° and 45° as a compromise between a high incidence angle for best linearity of the imaging mechanism and a steep incidence angle for high backscattered power. The wind speed and, in particular, the wind direction are important parameters, which determine the mean offset of measured ATI phases as well as the linearity of the imaging mechanism. The wind vector should thus be known as accurately as possible. To some extent, it can be determined from the ATI dataset itself by analyzing measured SAR image intensities.
- To measure two-dimensional current fields, dual-beam SARs with two different look directions can be used, or the SAR can be operated in spotlight mode. If the corresponding hardware is not available, one can combine data from ascending and descending overflights statistically or use hydrodynamic models to retrieve the along-track component of the current field from the measured cross-track component and additional information, such as the bottom topography. Some applications, such as river outflow monitoring or the retrieval of bathymetric maps from ATI data, can be based on one-dimensional measurements alone if two-dimensional data are not available.
- Also cross-track interferometry (XTI) can be used over water to obtain information on geostrophic currents and other phenomena which are associated with mesoscale sea level variations. An accuracy of about 1 cm can be achieved at a spatial resolution on the order of kilometers, which is comparable to the performance of conventional radar altimeters. However, XTI can produce two-dimensional maps of the sea level with a swath width on the order of 100 km, where altimetry provides only point measurements along the satellite's ground track. Furthermore, XTI is less sensitive to variations of atmospheric parameters. Limitations of its applicability may only result from the fact that only spatial variations but no absolute sea levels can be measured.
- InSAR systems with combined along-track and cross-track baselines will basically work like pure XTI systems over land (where targets are not moving) and like pure ATI systems over water (where no pronounced topography is present). Our model results indicate that the mean effect of XTI phase variations associated with the elevation of surface waves is negligible when converting combined ATI / XTI phase images into current fields. Only altimetry with combined ATI / XTI data will be a delicate problem, since the small XTI phase variations associated with the mesoscale sea surface topography may be dominated by ATI phase variations with variations in the current field and the wave field on comparable spatial scales.

ACKNOWLEDGMENTS

The ATI phase images of Figure 3-7 were processed by Oliver Hirsch, University of Hamburg, at Aero-Sensing GmbH, Oberpfaffenhofen. The ADCP data of Figure 3-2 were provided by Holger Klein and Ernst Mittelstaedt, German Federal Maritime and Hydrographic Agency (BSH), Hamburg. The circulation model results shown in the same figure were provided by Norbert Winkel, German Federal Waterways Engineering and Research Institute (BAW), Hamburg. The figure was produced by Juliane Pestel, University of Hamburg. The EURoPAK experiment was financed by the German Federal Ministry of Education and Research (BMBF) through the German Aerospace Center (DLR), Bonn, under Grant No. 50 EE 9723.

REFERENCES

Alpers, W., Measurement of mesoscale oceanic and atmospheric phenomena by ERS-1 SAR, *URSI Radio Science Bulletin*, *275*, 14-22, 1995.

Essen, H.H., K.W. Gurgel, and T. Schlick, On the accuracy of current measurements by means of HF radar, *IEEE J. Oceanic Engineering*, *25*, 472-480, 2000.

Fischer, J., and N.C. Flemming, *Operational Oceanography: Data Requirements Survey*, *EuroGOOS Publication No. 12*, Southampton Oceanography Centre, Southampton, UK, 1999.

Frasier, S.J., and A.J. Camps, Dual-beam interferometry for ocean surface current vector mapping, *IEEE Trans. on Geosci. and Remote Sensing*, *39*, 401-414, 2001.

Goldstein, R.M., and H.A. Zebker, Interferometric radar measurement of ocean surface currents, *Nature*, *328*, 707-709, 1987.

Graber, H.C., D.R. Thompson, and R.E. Carande, Ocean surface features and currents measured with synthetic aperture radar interferometry and HF radar, *J. Geophys. Res.*, *101*, 25,813-25,832, 1996.

Horstmann, J., S. Lehner, W. Koch, and R. Tonboe, Computation of wind vectors over the ocean using spaceborne synthetic aperture radar, *Johns Hopkins APL Technical Digest*, *Vol. 21*, *No. 1*, 100-107, 2000.

Horstmann J., W. Koch, S. Lehner, and R. Tonboe, Ocean winds from RADARSAT-1 ScanSAR, submitted to *Can. J. Remote Sens.*, 2001.

Massonnet, D., Capabilities and limitations of the Interferometric Cartwheel, presented at CEOS SAR Workshop, Toulouse, France, October 1999, available at http://www.estec.esa.nl/CONFANNOUN/99b02/index.html, 1999.

Massonnet, D., E. Thouvenot, S. Ramongassié, and Laurent Phalippou, A wheel of passive radar microsats for upgrading existing SAR projects, in *Proc. 2000 International Geoscience and Remote Sensing Symposium (IGARSS 2000)*, 1000-1003, Inst. of Elec. and Electron. Eng., Piscataway, N.J., USA, 2000.

Ramongassié, S., L. Phalippou, E. Thouvenot, and D. Massonnet, Preliminary design of the payload for the Interferometric Cartwheel, in *Proc. 2000 International Geoscience and Remote Sensing Symposium (IGARSS 2000)*, 1004-1006, Inst. of Elec. and Electron. Eng., Piscataway, N.J., USA, 2000.

Romeiser, R., and W. Alpers, An improved composite surface model for the radar backscattering cross section of the ocean surface, 2. Model response to surface roughness variations and the radar imaging of underwater bottom topography, *J. Geophys. Res.*, *102*, 25,251-25,267, 1997.

Romeiser, R., and D.R. Thompson, Advanced modeling of microwave Doppler spectra and along-track interferometric SAR signatures of ocean surface currents, in *Proc. 1999 International Geoscience and Remote Sensing Symposium (IGARSS '99)*, pp. 2604-2606, Inst. of Elec. and Electron. Eng., Piscataway, N.J., USA, 1999.

Romeiser, R., and D.R. Thompson, Numerical study on the along-track interferometric radar imaging mechanism of oceanic surface currents, *IEEE Trans. on Geosci. and Remote Sensing*, *38-II*, 446-458, 2000.

Romeiser, R., W. Alpers, and V. Wismann, An improved composite surface model for the radar backscattering cross section of the ocean surface, 1. Theory of the model and optimization / validation by scatterometer data, *J. Geophys. Res.*, *102*, 25,237-25,250, 1997.

Romeiser, R., S. Ufermann, and S. Stolte, Energy transfer between hydrodynamically modulated long and short ocean waves by interaction with the wind field, in *Proc. 1999 International Geoscience and Remote Sensing Symposium (IGARSS '99)*, pp. 965-967, Inst. of Elec. and Electron. Eng., Piscataway, N.J., USA, 1999.

Romeiser, R., S. Ufermann, and W. Alpers, Remote sensing of oceanic current features by synthetic aperture radar – achievements and perspectives, *Annals Telecom.*, in press, 2001.

Senet, C., J. Seemann, and F. Ziemer, The near-surface current velocity determined from image sequences of the sea surface, *IEEE Trans. on Geosci. and Remote Sensing*, *39*, 492-505, 2001.

Thompson, D.R., Calculation of microwave Doppler spectra from the ocean surface with a time-dependent composite model, in *Radar Scattering from Modulated Wind Waves*, edited by G.J. Komen and W.A. Oost, Kluwer Academic Publishers, Dordrecht, Netherlands, 27-40, 1989.

Thompson, D.R., and J.R. Jensen, Synthetic aperture radar interferometry applied to ship-generated waves in the 1989 Loch Linnhe experiment, *J. Geophys. Res.*, *98*, 10,259-10,269, 1993.

Ufermann, S., and R. Romeiser, A new interpretation of multifrequency / multipolarization radar signatures of the Gulf Stream front, *J. Geophys. Res.*, *104*, 25,697-25,706, 1999a.

Ufermann, S., and R. Romeiser, Numerical study on signatures of atmospheric convective cells in radar images of the ocean, *J. Geophys. Res.*, *104*, 25,707-25,720, 1999b.

Valenzuela, G.R., Theories for the interaction of electromagnetic and ocean waves – A review, *Boundary Layer Meteorol.*, 13, 61-85, 1978.

Wunsch, C., and D. Stammer, Satellite altimetry, the marine geoid, and the oceanic general circulation, *Ann. Rev. Earth Planet. Sci.*, *26*, 129-253, 1998.